PROCEEDINGS, 49th Workshop on Geothermal Reservoir Engineering
Stanford University, Stanford, California, February 12-14, 2024
SGP-TR-227

Greenfield Reservoir Engineering for the Wattenberg Field with Comparison of Advanced, Enhanced, and Caged Geothermal Systems

Luke P. Frash, Meng Meng, Bijay K C

Earth and Environmental Sciences Division, Los Alamos National Laboratory, Los Alamos, NM, USA

lfrash@lanl.gov

Keywords: Enhanced Geothermal Systems, Advanced Geothermal Systems, Caging, Technoeconomics

ABSTRACT

New and improved methods to extract energy from hot dry rock are becoming available and, if successful, they could unlock terawatts of energy production from previously untapped resources. Three promising methods include enhanced geothermal systems (EGS), advanced geothermal systems (AGS), and caged geothermal systems (CGS). EGS uses particle propped hydraulically stimulated fractures to convey fluid through low permeability rock to extract heat. AGS uses closed loop flow through an array of deep wells to extract heat without a need for hydraulic stimulation. CGS uses boundary wells to contain high-pressure propped hydraulic fractures while minimizing seismic risk. However, each of these methods comes with its own challenges. EGS risks low production due to proppant degradation and rapid thermal short circuiting. AGS risks extreme capital costs for well drilling and low rates of heat extraction. CGS risks the unproven caging concept and extreme pumping costs. Here, we seek to forecast the performance of each method in an ultra-high uncertainty greenfield scenario that includes natural fractures. Our target site is the Wattenberg geothermal anomaly near Fort Collins, Colorado. Using our open-source Geothermal Design Tool (GeoDT) with only basic input data, we completed a stochastic power and economic risk assessment for future 6 km deep wells. In the conduction-dominated Wattenberg anomaly, we anticipate bottom hole temperatures in the range of 220 to 300 °C. Subsurface stress and fault conditions are unknown. Rock properties are unknown aside from the basement likely consisting of igneous or metamorphic rock. Our analysis predicts that CGS with an 'X'-pattern of five wells (i.e., XGS) holds the greatest promise for economic heat production at 99 to 220 $USD/MWh, followed by three well EGS at 87 to 2200 $USD/MWh, and then 25-loop AGS at 410 to 860 $USD/MWh.

1. INTRODUCTION

The Wattenberg geothermal anomaly is located in Weld county near Fort Collins, Colorado (Figure 1). This location is known to have a high thermal gradient that we estimate in the range of 26 to 50 °C/km. The basement is thought to be granitic or gneissic but confirmatory data is lacking. Pending well data, the minimum principal stress is hoped to have an uncertainty of ±15° with a possible orientation of 75° AzN. No further site-specific data was employed for this study. Two 6 km deep exploratory wells have been proposed for this site as part of the Geothermal Limitless Approach to Drilling Efficiencies (GLADE) project, funded by the US Department of Energy's Geothermal Technologies Office. Drilling is planned circa 2025. We seek to optimize well placement before site-data is obtained.

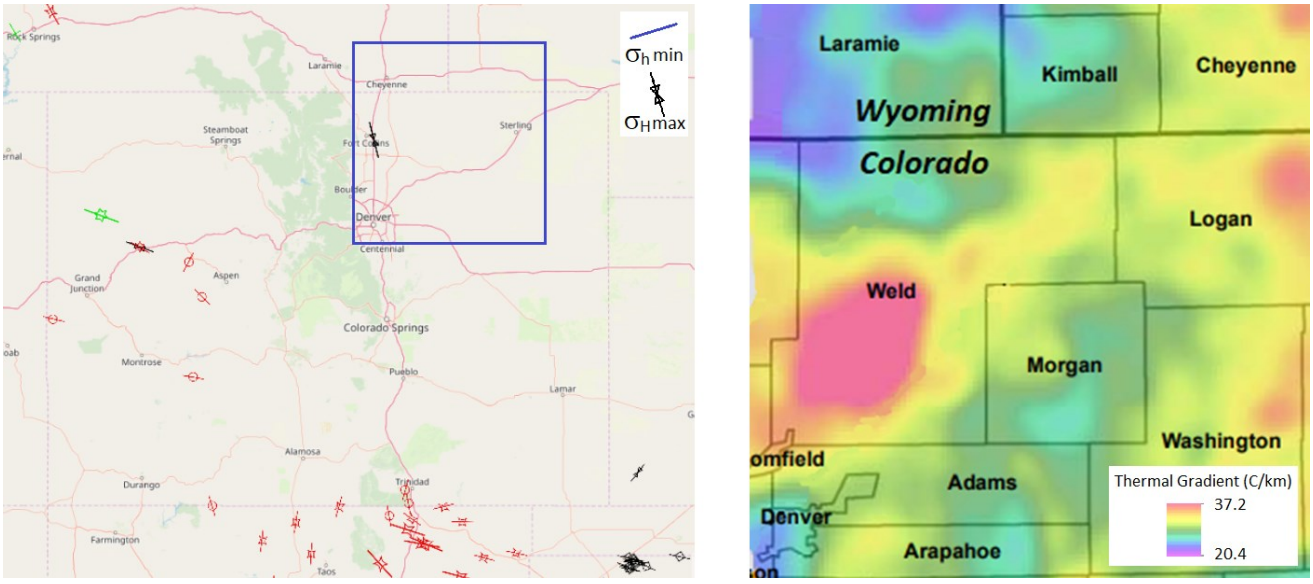

Figure 1: The Wattenberg geothermal field is a greenfield resource. Stress data is from World Stress Map (Heidbach, 2018) and the heat data is from a master's thesis (Thul, 2012; Förster and Merriam, 1997). Other model input data was compiled from general non-site-specific sources, including our own laboratory data for fracture properties.

To develop this geothermal resource for electrical power generation, we will consider four different strategies (Figure 2). First, we consider Advanced Geothermal Systems (AGS) which is a closed-loop multi-lateral concept where a sealed tube heat exchanger is constructed inside of a geothermal resource. This approach offers the benefit of negligible fluid losses, negligible risk of injection induced seismicity, relatively predictable performance, and suitability for working fluids other than water if so desired. However, the commercial length of drilling with 25-loops at 6 km depth totals at around 150 km, based on our analysis. Second, we consider Caged Geothermal Systems (CGS) which is a new concept where boundary wells are drilled to encircle an injection well with the goal of capturing and containing both the injected fluid and any fractures that are stimulated (Frash et al., 2020). This method holds promise to allow sustained injection at high-rate, high-pressure, and long-durations while simultaneously limiting injection induced seismic risk. However, this concept has not been proven in practice and it requires drilling at least four wells. Third, we consider Enhanced Geothermal Systems (EGS) which is the first concept that was ever field tested for hot dry rock geothermal energy extraction (Duchane and Brown, 2002). This concept uses at least two wells and hydraulic stimulation with proppant particles and/or natural fracture shear stimulation to facilitate fluid circulation through relatively impermeable rock. However, this method has struggled to make its way into practice because of its risk of thermal short circuits (i.e., premature cooling of the produced fluid), injection induced seismicity, and the expectation that proppants are unlikely to withstand temperatures that could exceed 200 °C for long durations. In addition, challenges include high temperature drilling, the high uncertainty associated with subsurface conditions, and an abundance of competing energy technologies that require less capital to demonstrate (e.g., wind, solar, and natural gas). Fourth, we propose XGS as a hybrid EGS-CGS five-spot concept that uses proppants and caging together along with in-well flow proportioning (i.e., flow rate control). This concept would be well-suited for upscaling via large patterns of injection and production wells that could be expanded laterally or vertically to increase the output and longevity of a hot dry rock geothermal plant. However, the required technology for in-well flow control has not been adequately developed. Our key goals for evaluating each technology include identifying optimized flow rates, well spacing, well orientation, and numbers of wells. In addition, we seek to forecast the risk of low performance due the influence of natural fractures, heterogeneity, and seismic slip.

2. MODEL SETUP

Now, let us concisely describe the setup of our stochastically predictive model that includes three-dimensional fracture networks, fracture stimulation, geomechanics, flow, heat transport, power production, and economic valuation – all while site-specific data is absent. Assuming that such a model cannot be precise would be wise, however low precision does not preclude usefulness nor does it preclude accuracy with respect to decision making when uncertainty is high. Crucially, in high-uncertainty scenarios such as ours, there is a strong temptation to circumvent complexity by using assumptions of homogeneity, such as by excluding natural fractures and faults. Such a simplified approach would help make the modeling work easier, but it would be ignorant since a lack of information does not equate to a lack of complexity. Our Geothermal Design Tool (GeoDT; Frash, 2021) incudes natural fractures, uncertain stresses, heterogeneous fracture properties, and variable subsurface conditions by default. When executed in large ensembles of 100's to 1000's of realizations, we expect that our high-uncertainty approach should yield accurate guidance with respect to reservoir design optimization. Unfortunately, no tool yet exists to validate our approach end-to-end, given that we model shear and tensile fracture stimulation at the reservoir scale with project lifespans greater than 10 years, but we nonetheless trust that our approach should be effective in the interim.

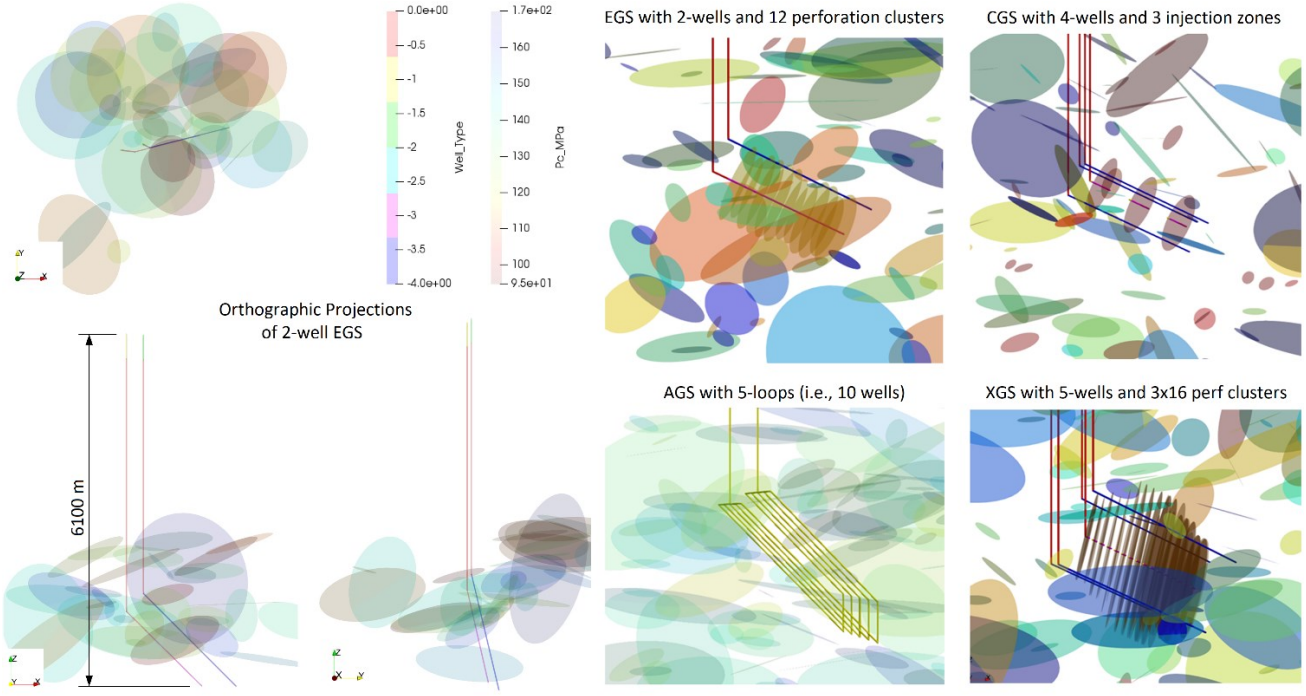

Figure 2: Model setup with 6.1 km total depth injection wells having 1600 m inclined segments drilled at 25° dip toward the ENE. Key design variables included flow rate, well spacing, number of wells, number of perforation clusters, and number of isolated injection stages. Multiple isolated injection stages appear as a dashed-line. One hydraulic fracture is assumed per perf-cluster. Development strategies included AGS, EGS, CGS, and XGS.

Our study considers a fixed total vertical depth for an injection well at 6.1 km, based on the proposed drilling plan for GLADE (Figure 2). Primary design variables for decision making include well spacing (i.e., the distance between the injector and producer wells) and circulation flow rate. In addition, the number of wells, number of stimulation stages, and number of AGS flow-loops was varied between batches of ensembles, having up to 3,000 realizations each. Secondary design variables included the length, dip, and direction of the inclined section of the wells (i.e., the directionally drilled segment), but these values were fixed across all realizations since we anticipated only minor gains in performance from optimizing these terms based on our prior work (Frash, 2021; Frash, 2022; Frash et al., 2022; Frash et al., 2023). However, we must point out that orienting the wells to be near parallel to the minimum principal stress is known to be critical for enhanced and caged geothermal systems because multiple transverse hydraulic fractures are needed to efficiently extract heat from the reservoir. Therefore, a diagnostic fracture injection test is assumed to be part of the drilling plan in order to measure the in-situ stress directions and then properly orient the well. Such tests can reasonably achieve directional uncertainty in the vicinity of ±15° for this critical parameter.

Our model includes more than 71 parameters to characterize the rock, fractures, wells, power plant, and economic metrics (Table 1). Nearly all of these parameters are randomly sampled from uniform or log-uniform distributions. It is impractical to elaborate on all model details in this paper, so readers are referred to the GitHub repository for GeoDT for details and the included "GLADE" script that was used for this study. Additional information regarding the model and its validation can be found in our prior publications and the GitHub documentation (Frash, 2021). However, this model is in active development so the documentation is not comprehensive nor complete. Questions, clarifications, or concerns can be directed to the author using the contact information above. In total we modeled 16 design variants with up to 3,000 realizations each, requiring 3 days to complete using a desktop computer.

Table 1: Model parameters used for this study.

Parameter	Variable	Min	Max	Unit
***Production Well Count	w_count	1	4	ea
***Well Phase	w_phase	90	270	deg
***Perforation Clusters	perf_clusters	3	48	ea
***Sand to Water Concentration	sand	0	0.044	m3/m3
***Well Intervals	w_intervals	1	16	ea
***Well Spacing	w_spacing	50	700	m
***Target Injection Rate	Qinj	0.01	1.00	m3/s
Reservoir Size (Half)	size	2500	2500	m
Model Thermal Gradient?	gradient	TRUE	TRUE	T/F
Reservoir Depth	ResDepth	6100	6100	m
Thermal Gradient	ResGradient	36	50	C/km
Rock Density	ResRho	2550	2950	kg/m3
Rock Thermal Conductivity	ResKt	2.27	3.58	W/m2
Rock Specific Heat Capacity	ResSv	0.74	1.2	kJ/kg-K
Surface Temperature	AmbTempC	0	0	C
Surface Pressure	AmbPres	0.101	0.101	MPa
Rock Young's Modulus	ResE	55	62	GPa
Rock Poisson's Ratio	Resv	0.26	0.4	
Minimum Earth Stess Coef.	Ks3	0.3	0.8	Pa/Pa
Intermediate Stress Coef.	Ks2	0.4	1.1	Pa/Pa
Minimum Stress Azimuth	s3Azn	60	90	deg
Azimuth's Uncertainty	s3AznVar	0.75	0.75	deg
Minimum Stress Dip	s3Dip	0	30	deg
Dip's Uncertainty	s3DipVar	0.75	0.75	deg
Fracture Count Set 1	fNum	40	80	
Fracture Count Set 2	fNum	20	40	
Fracture Count Set 3	fNum	10	20	
Fracture Diameter	fDia	200	2000	m
Fracture Slip-Length Scaling	gamma	0.001	0.063	m/m
Fracture Dilation-Slip Scaling	a	0	0.13	m/m
Fracture Hydraulic-Dilation Scaling	N	0	2	m/m
Fracture Compressibility	alpha	2.00E-09	1.00E-07	1/Pa
Proppant Compressibility	prop_alpha	2.00E-09	1.00E-07	1/Pa
Fracture Initial Hydraulic Aperture	bh	1.00E-08	1.00E-04	m
Boundary Hydraulic Aperture	bh_bound	1.00E-04	1.00E-03	m
Fracture Stranding Scale Factor	f_roughness	0.125	1	m/m

Parameter	Variable	Min	Max	Unit
Well Inclined Azimuth	w_azimuth	75	75	deg
Well Inclined Dip	w_dip	25	25	deg
Well Inclined Proportion	w_proportion	0.8	0.8	m/m
Well Inclined Length	w_length	2000	2000	m
Casing Inner Radius	ra	0.1397	0.1397	m
Casing Outer Radius	rb	0.1524	0.1524	m
Borehole Radius	rc	0.1778	0.1778	m
Well Hydraulic Roughness	rgh	80	80	
Cement Thermal Conductivity	CemKt	2	2	W/m2
Cement Specific Heat Capacity	CemSv	2000	2000	kJ/m3-K
Generator Efficiency	GenEfficiency	0.85	0.85	
Lifespan of Production	LifeSpan	15	15	yr
Production Wellhead Pressure	p_whp	1	1	MPa
Injection Temperature	Tinj	20	90	C
Convection Coefficient	H_ConvCoef	3	3	
Water Density	PoreRho	920	932	kg/m3
Water Viscosity	Poremu	0.2	0.2	cP
Proppant Pack Conductivity	kf	10	10	um2cm
Perforation Diameter	perf_dia	0.015	0.015	m
Perforations per Cluster	perf_per_cluste	3	3	
Production Well Drawdown	dPp	0	0	MPa
Solver's Pressure Increment	dPi	0.02	0.02	MPa
Maximum Injection Pressure*	pfinal_max	0.9	0.9	s3
Fracture Friction Angle	phi	30	50	deg
Fracture Cohesion	mcc	1	6	MPa
Hydraulic Fracture Cohesion	hfphi	15	35	deg
Hydraulic Fracture Friction Angle	hfmcc	0.1	0.4	MPa
Electric Sales	sales_kWh	0.1372	0.1372	$/kWh
Drilling Cost	drill_m	2763.06	2763.06	$/m
Drill Pad Cost	pad_fixed	5.90E+05	5.90E+05	$
Power Generation Cost	plant_kWe	2025.65	2025.65	$/kW
Exploration Cost (Geophysics)	explore_m	2683.41	2683.41	$/m
Operation Cost (Maintenance)	oper_kWh	0.03648	0.03648	$/kWh
Earthquake Penalty (Coefficient)	quake_coef	2.00E-04	2.00E-04	$/Mw
Earthquake Penalty (Exponent)	quake_exp	5	5	$/Mw

*Applies to EGS scenarios only, *** design parameter

3. ENSEMBLE RESULTS AND OPTIMIZATION

Visualizing and interpreting 16 batches of 3,000 realizations of transient power production from three-dimensional fracture flow and transport models is not a trivial task. Here, we use an example from our 25-loop AGS ensemble (Figure 3) to explain our workflow so that the compiled results will have more context. The geometry of the AGS wells excludes the curvature of actual deviated wells because such details have a negligible effect on our final results. Wells in the AGS models were broken into segments to more accurately predict thermal drawdown behavior given that rock temperature will vary with depth. Thermal gradients are a new feature that was added to GeoDT to enable evaluation of AGS, but the radial heat flow model for wells has been in GeoDT since its first release. Other improvements to GeoDT that were implemented for this study include: a routine to identify critically oriented orthogonal natural fractures using stress tensors; and improvements to the flow solver to better account for casing perforation effects and fracture geo-hydro-mechanics.

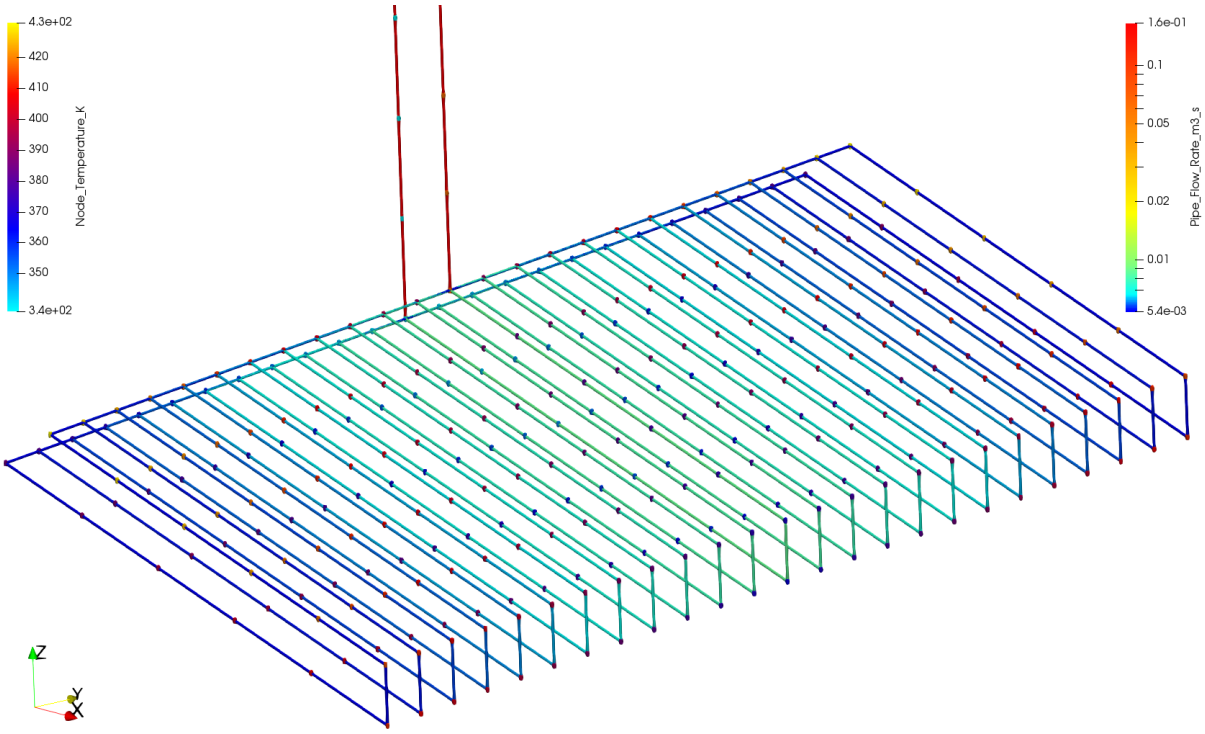

Figure 3: AGS design variant with 25-loops (i.e., 50-wells) at a nominal well spacing of 220 m and total injection rate of 0.164 m^3/s exhibiting nonuniform flow through the loops at 0.005 to 0.008 m^3/s due to flow mechanics. Faster flowing loops extract heat faster but produce at lower temperatures over time. Optimization using a range of boundary conditions is needed to ensure a good flow rate is selected to maximize the economic performance of each design variant.

As shown (Figure 3), the flow solver identifies that the longer flow paths for outer wells will have lower flow rates than the inner wells due to the associated increase in hydraulic resistance. This heterogeneity in flow complicates design optimization and is a behavior that will occur in the field. The slower flow in the outside wells results in hotter produced fluids, but this heat is then diluted by mixing with the faster flowing and colder inner wells. At the lowest injection rates, the produced fluid temperature will be nearly equal to the ambient surface temperature because the fluid cools as it rises in the production well. At the highest flow rates, the produced fluid will also be cold and nearly equal to the injection temperature because it will have inadequate residence time to heat up in the reservoir. Increasing the number of loops helps to increase residence time for heating and to mitigate cooling as the fluid rises, but it does not solve the effects entirely. We completed a large ensemble of models to identify the optimum injection rate, well spacing, and number of wells for AGS, EGS, CGS, and XGS. The optimum flow rate is that which yields the highest electrical energy production potential, averaged over the lifespan of the project. We have found that enthalpy decline over time (Figure 4) is a common trait among all optimized flow rates because larger thermal gradients equate to higher heat flow. We have also found that the optimum injection rates tend to fall into the range of 0.01 to 1.0 m^3/s. The lower end of this range produces power too slowly to offset the capital cost, assuming that the wells will become unusable after 15 years due to corrosion and scale. The higher end of this range requires very large wells (e.g., >0.35 m diameter) to prevent the excessive pumping losses that also lower performance. Ultimately, insights of this type highlight the value of a stochastic solver that can evaluate the complicated interactions between disparate mechanisms to identify the most promising methods for geothermal energy development.

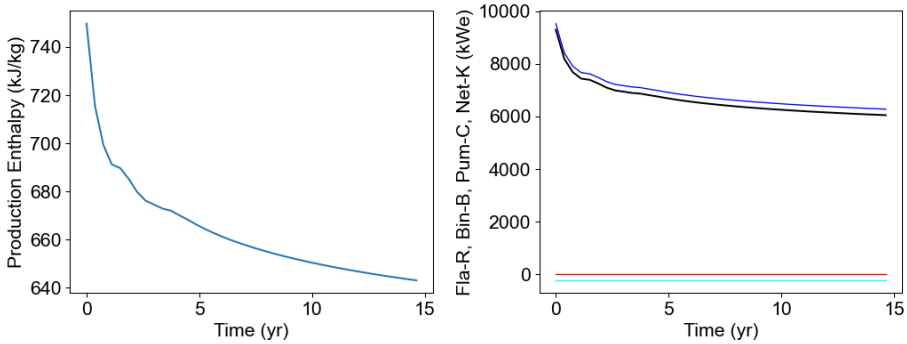

Figure 4: Thermal decline with time is a common trait among optimized AGS, EGS, CGS, and XGS designs. However, this rate of decline cannot be too fast or the economics will suffer. This example is from the models shown in Figure 3. Power analysis includes flash Rankine (Fla-R: Red), isobutane binary (Bin-B: Blue), and pumping losses (Pum-C: Cyan) to estimate the combined net power production (Net-K: Black).

Visualizing thousands of power production timeseries and three-dimensional graphics would be ineffective for design optimization and comparative evaluation. Relatedly, including non-optimum flow rates when comparing designs would introduce unwanted bias, leading to incorrect conclusions. To facilitate comparison, we calculate the non-negative net average power production per year (kW) for each realization along with the associated net present value ($), yielding one datapoint per realization. We find that net present value is an exceptionally useful metric for comparing designs, but it is also a misleading metric for actualized profits because too many nuances are excluded, such as tax credits. A statistically comprehensive optimization with large ensembles to yield smooth self-consistent probability distributions is not our goal because such an effort would create to a false sense of confidence in small differences. Caveats aside, optimized design parameters ranges for each batch of realizations (Table 2) were estimated using plots of injection rate, well spacing, average power production, and net present value (Figure 5). We apologize that showing the optima selection for each of the 16 batch models on their respective scatterplots is beyond the scope of this document. However, we trust that this approach to optimization is agreeable with respect to the high-uncertainty associated with greenfield geothermal reservoir design.

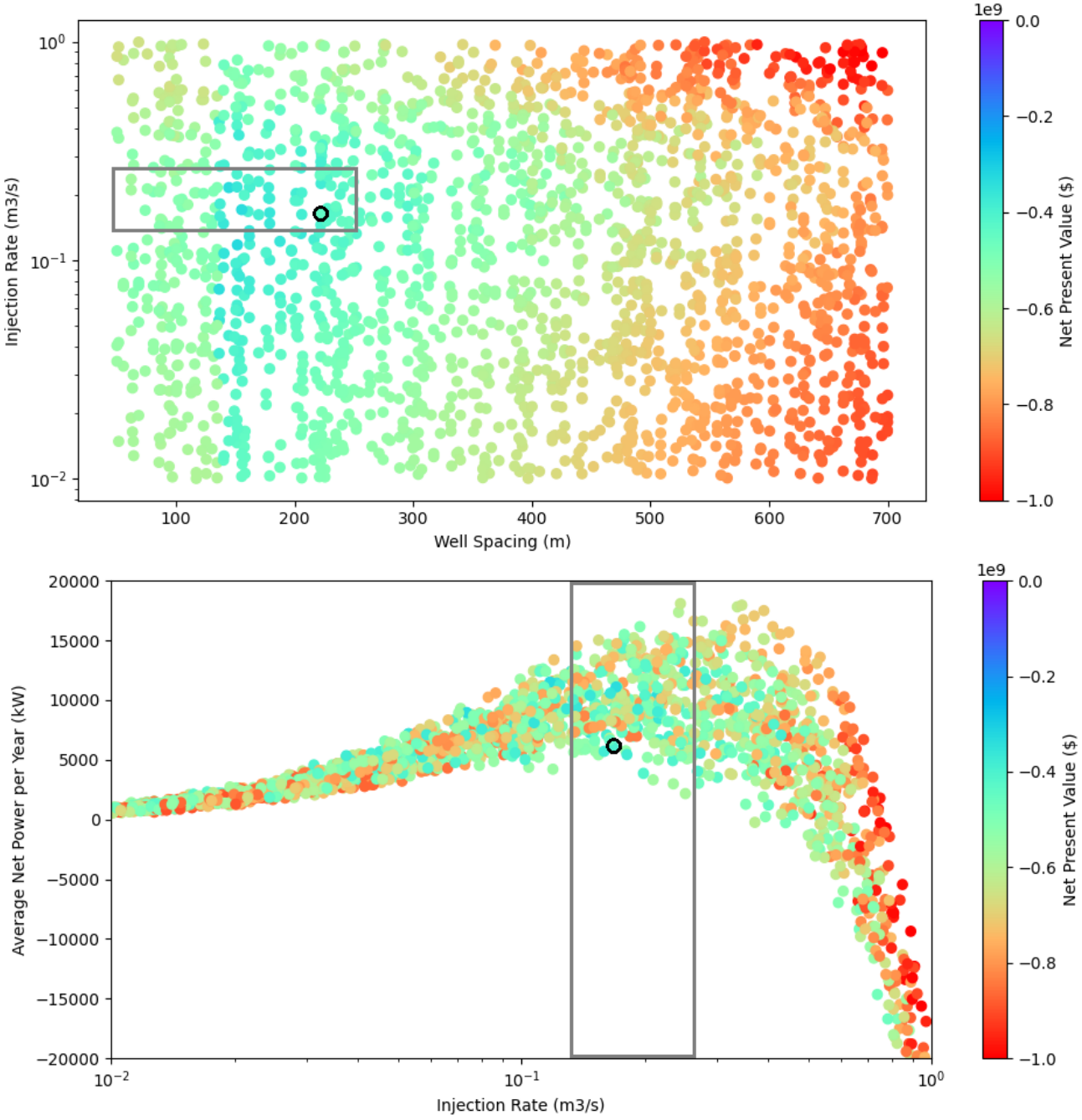

Figure 5: Example 3D scatterplots used to estimate optimized designs for 25-loop AGS showing peak potential in the range of 0.13 to 0.26 m^3/s injection rate and 50 to 250 m well spacing. This plot includes 2061 realizations, 87 of which fall within the optimized range. A black circle highlights the realization from Figures 3 and 4.

Table 2: Optimized flow rate and well spacing for each design variant.

Model	Realizations	Flow Rate (m^3/s)	Spacing (m)
AGS – 1 loop	3143 (140)	0.02 – 0.04	50 – 250
AGS – 5 loop	2479 (122)	0.03 – 0.06	50 – 250
AGS – 13 loop	3000 (177)	0.06 – 0.13	50 – 250
AGS – 25 loop	2061 (87)	0.13 – 0.26	50 – 250
CGS – 4 well 3 stage	3000 (186)	0.08 – 0.20	450 – 650
CGS – 4 well 6 stage	3000 (352)	0.08 – 0.40	450 – 650
CGS – 4 well 9 stage	3000 (378)	0.08 – 0.50	450 – 650
EGS – 2 well 6 stage	3000 (252)	0.02 – 0.06	450 – 650
EGS – 2 well 12 stage	3000 (221)	0.03 – 0.08	450 – 650
EGS – 2 well 24 stage	3000 (164)	0.04 – 0.10	450 – 650
EGS – 2 well 48 stage	3000 (375)	0.04 – 0.20	450 – 650
EGS – 3 well 48 stage	3000 (259)	0.07 – 0.33	450 – 650
EGS – 4 well 48 stage	1060 (113)	0.07 – 0.42	450 – 650
XGS – 5 well 3x4 stage	3000 (195)	0.08 – 0.22	450 – 650
XGS – 5 well 3x8 stage	636 (71)	0.10 – 0.36	450 – 650
XGS – 5 well 3x16 stage	622 (61)	0.12 – 0.55	450 – 650

Note: The number of optimized realizations filtered from each ensemble is given in parentheses.

4. HETEROGENEITY IN FRACTURES AND SHORT CIRCUITS

Our solver applies uncertainty across all subsurface parameters with the goal of averting perfectly impossible solutions. Numerical instability caused by "infinitely conductive" hydraulically propped fractures flowing into open wells and the instability caused by the severe discontinuity in the hydraulic properties of one fracture versus another, is not trivial nor negligible. We seek the 'ugly' solutions where heterogeneity can and will cause short circuiting. Simultaneously, we desire solutions that are physically meaningful and plausible. To emphasize how this applies to an EGS design, we provide a random sample from the 2-well 48 stage ensemble (Figure 6). This result, just as it's companions, it not assumed to be numerically accurate and precise. Instead, we seek phenomenological understating to better assess the effect of high-level design decisions on complex reservoir processes. For example, we can evaluate the effectiveness of reducing perforation size on increasing flow uniformity at the same time as evaluating its effect on parasitic losses due to increased pumping pressures. Using this understanding, we can then better evaluate the cascading effect on economic feasibility. Every one of our 40,000 realizations has accompanying timeseries and 3D data to aid users of this tool in understanding how design choices could influence productivity. Unfortunately, including those examples here would yield a document more than 40,000 pages long, which is obviously impractical for a conference paper. Instead, we provide only this single random example of how heterogeneity causes non-uniform fracture growth and non-uniform distribution of flow through fractures in EGS (Figure 6). When viewing this result, the flow rates are shown in the pipes of the pipe-and-node model that we use to estimate flow through networks of wells and fractures. These pipes are visually represented as lines, but the flow through them is calculated using the stress-dependent, shear-dependent, and proppant-dependent hydro-mechanical properties of their corresponding fractures.

5. COMPARISON OF METHODS

The usefulness of GeoDT batch ensembles is revealed when employed to compare designs in high uncertainty scenarios. We prefer to accomplish this by calculating quantiles from the optimized designs. This approach can be contrasted with filtering by performance or other metrics without regard to the controllable design decisions. Our experience employing GeoDT for the PIVOT Geothermal Datathon in 2022 and 2023 revealed that filtering out low performance scenarios directly, without regard for the associated design, was a common alternative approach to the analysis of ensemble results. However, we profess that such an approach is invalid because it fails to account for low-performing scenarios that can occur even if the design is optimized. These low performing scenarios are often linked to natural fractures that caused short circuiting, low fracture conductivity, high leakoff, or large induced seismic events. The best designs for geothermal power production will maximize economic potential while minimizing risk for the maximum number of realizations. In other words, we predict that economic failure is possible even when the best development approach is used.

For this study, let us first inspect the 5%, 10%, 50%, 90%, and 95% quantiles with respect to net power output (Figure 7). This prediction forecasts AGS as the lowest risk design with good performance, where the uncertainty mostly stems from the uncertain temperature of the reservoir at 6.1 km depth, ranging from 220 to 300 °C. Increasing the number of loops equates to higher production potential, as expected. XGS is a strong contender with even higher peak and nominal power potential when implemented with a high number of flow-controlled intervals (e.g., 16), but current technology is unable to achieve such high-fidelity flow control in the injection well. 9-stage CGS and 3-well EGS are similarly performing options, both with some risk of losses and high performance uncertainty. Increasing the number of wells generally associates with higher power output, but will be accompanied by higher cost. Likewise, more stimulation stages yields with higher output, especially if flow control is implemented during circulation. However, sole reliance on net power production would be unwise because the cost of development is also key to the favorability of a given design.

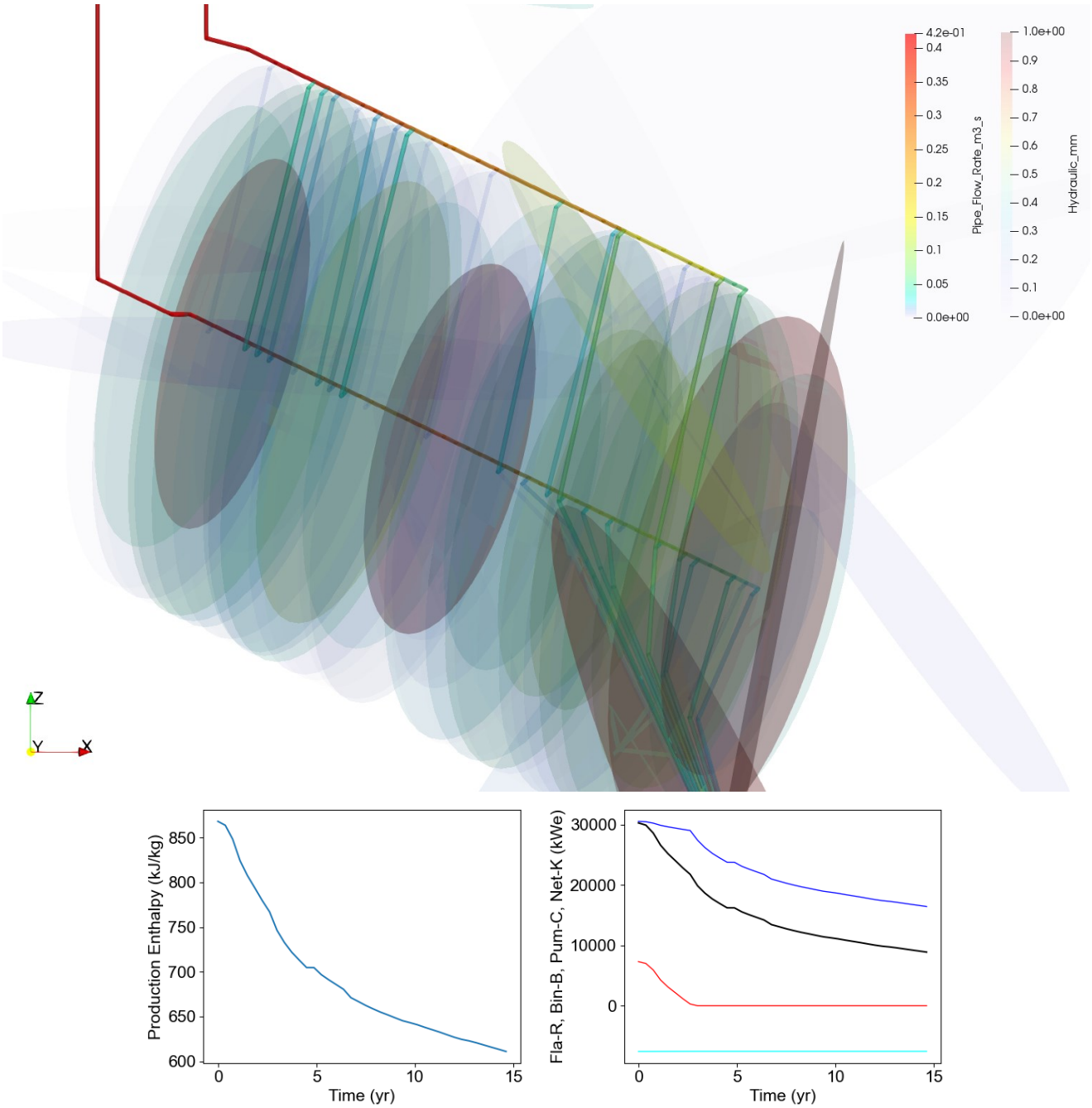

Figure 6: Example depicting fracture property and flow heterogeneity in a random realization from the 2-well 48-stage EGS ensemble. A fraction of the stimulated fractures connect to the production well due to this heterogeneity. Some fractures short circuit via an intersecting fault below the injection well. The geometry and hydraulic apertures of fractures were predicted using our coupled hydro-mechanical solver. The result is non-uniform flow with the understanding that this should better represent the impact of a multitude of complex subsurface processes, without needing to explicitly model each. Key to this, we do not require data that is unavailable nor data that is unobtainable.

Next, we inspect the quantiles for net present value (Figure 8) which will cause the narrative for "best design" to change dramatically. From this perspective, we can now see that AGS is currently far from economic with losses of at least $350M predicted for the 25-loop design and losses scaling proportionally to the number of loops. This low favorability for AGS stems from the high cost of drilling at 2760 $/m and the large amount of drilling that would be required. Profits would only be realized if the cost of drilling could be reduced by >90%, electricity sales increased by >300% from 13 ¢/kWh, or some other external factor shifted the favorability. In contrast, XGS outshines the competition with the highest net present value and lowest economic risk, but achieving such an outcome would require the development of an in-well flow proportioning technology that does not currently exist. Furthermore, XGS and CGS both rely on 'fracture caging' for fracture, flow, and seismicity control (Frash et al., 2020) which is yet another unproven concept at the field scale. Based on this analysis, EGS could be seen as the most realistic option but it is not without a risk of triggering large earthquakes and it also brings a risk of low performance due to short circuits or the inability to achieve an optimized injection rate due to low injectivity.

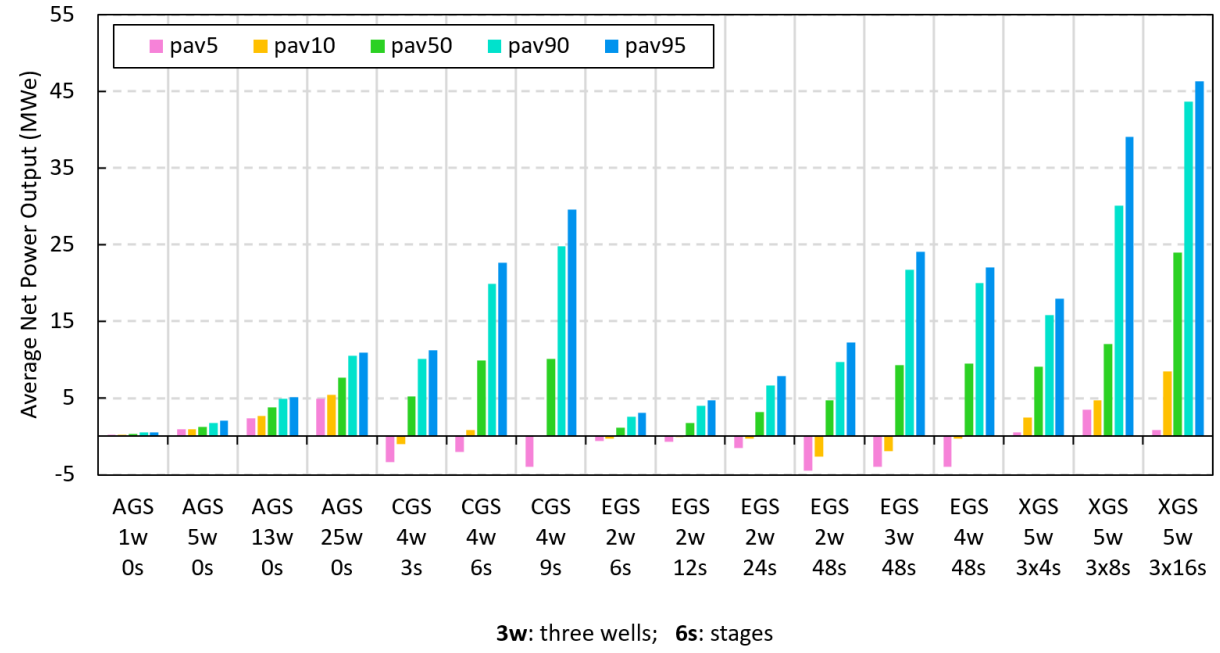

Figure 7: Average net power production per year (i.e., generated power – less pumping power) viewed using quantiles (e.g., pav90 signifying that 90% of the population had a lower value). AGS with 25-loops exhibits the lowest uncertainty and a high production potential. XGS with 3 per-clusters in each of 16 stages (i.e., 3x16) is revealed as a high-output powerhouse with relatively low risk. EGS and CGS show a high uncertainty along with poor to good power potential.

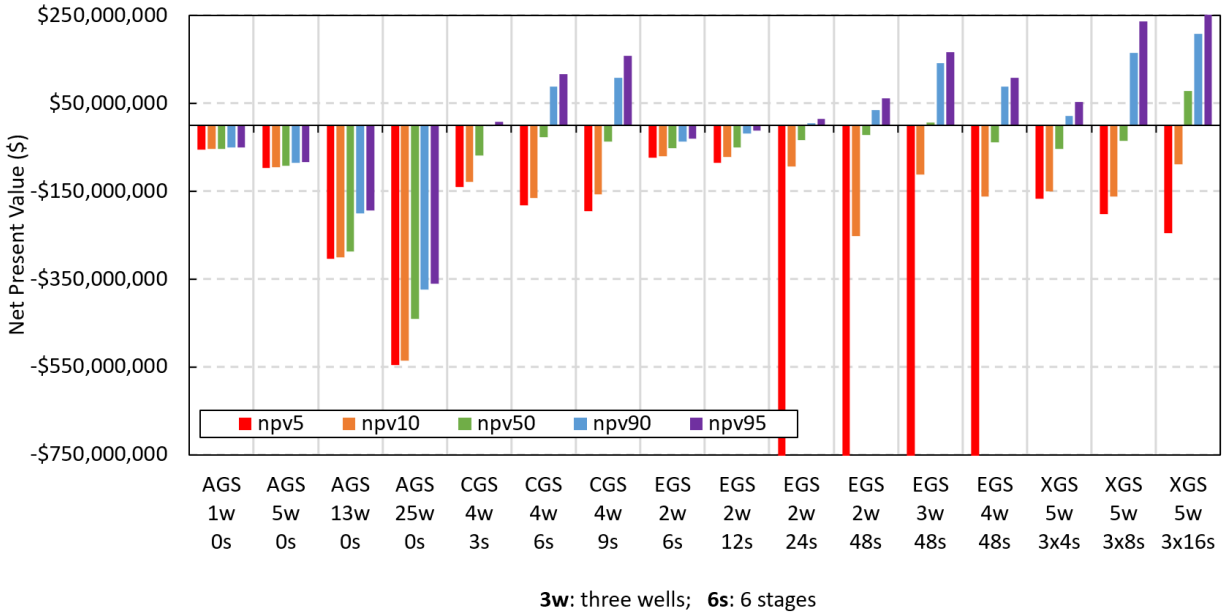

Figure 8: Net present value quantiles for each design. AGS is revealed to be very unfavorable for electrical power generation. EGS is revealed to have significant risk in around 10% of the realizations due to the short circuits and injection induced seismicity. CGS doesn't perform much better despite its lower risk of high losses. XGS outperforms all others with more than 50% of the realizations yielding a small profit in this highly uncertain greenfield scenario.

Using cost per megawatt-hour (Figure 9), provides one more perspective to compare these methods of geothermal energy development. The finding here was similar to what was revealed by net present value, but the low performance scenarios appear scarier and the high-performance scenarios become obscured because of the power-law scaling inherent to this metric. Most notably, low performance systems can have infinite cost per megawatt-hour. However, this metric provides a useful value for relating geothermal energy production to alternative technologies such as solar and wind. We explore this more in the next section.

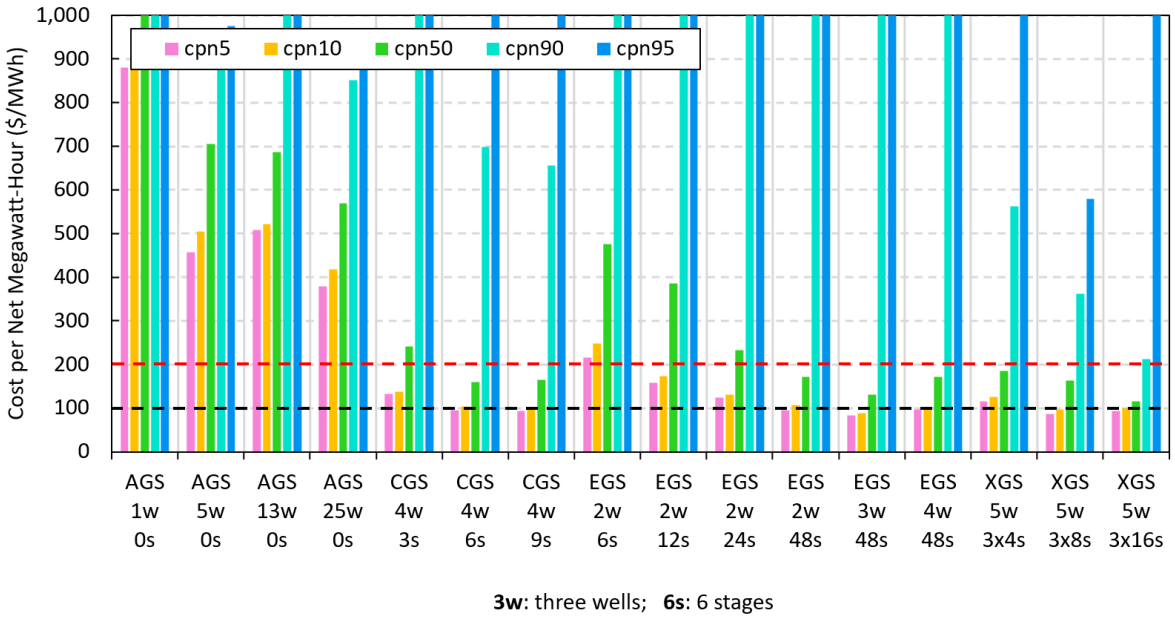

Figure 9: Cost per megawatt-hour for each design. A target of 100 $/MWh indicates cost competitiveness with other baseload energy technologies while a feasibility ceiling can be thought of as 200 $/MWh. AGS is again unfavorable by this metric. XGS appears to be promising and competitive, but only if its requisite core concepts of fracture caging and in-well flow proportioning can be achieved. EGS remains a promising approach, but only if the risk of injection induced seismicity can be proactively prevented or mitigated.

6. DISCUSSION

Our forecast predicts that XGS (i.e., EGS-CGS with 5-wells drilled before stimulation and with in-well flow proportioning) could be cost-competitive with alternative electrical energy technologies in the Wattenberg geothermal field (Figure 10). In addition, this energy would be clean, stable, low-risk, and generally independent of weather. Favorability would improve even further if the site was located near a customer that could benefit from low-enthalpy heat in the range of 50 to 120 °C, such as for district heating, spas, and greenhouses. Using this heat would notably offset emissions from gas furnaces and the like. If the seismic control aspect of XGS and CGS can be proven, they could be safely located closer to customers to decrease losses and thereby increase the economic benefits. Otherwise, AGS would remain the most viable option for energy generation within population centers. However, for AGS to be feasible, current drilling costs would need to be reduced by at least 90% or the market price for electricity would need to skyrocket by more than 300%.

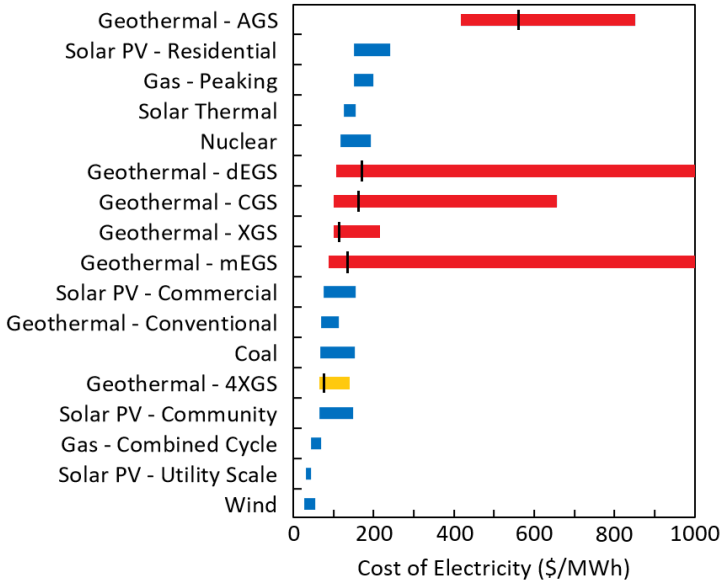

Figure 10: Greenfield forecast for the cost of electricity at Wattenberg geothermal anomaly compared to other energy technologies. Published values from Lazard (2019) are in blue. The 80% confidence intervals from this study are in red. An extrapolated value for 13-well XGS is shown in yellow. 'dEGS' signifies a classical EGS doublet with its two wells. 'mEGS' signifies EGS with more than two wells. Only the top performers from each concept are shown (c.f. Figure 9). Median (i.e., 50% quantile) values are indicated by black lines.

If operations were limited to a 2-well pilot study using only currently available technology, EGS offers the most promise at a nominal cost of 476 $/MWh. In contract, AGS would severely underperform relative to its cost at around 1324 $/MWh. Based on this price point, it unclear what role 2-well (i.e., doublet) AGS or EGS will have in the future. Furthermore, 2-well EGS would continue to be difficult to foster given its risk of generating damaging injection induced seismic events, occurring at a rate of around 1 in 10 in this study.

Given our findings, it seems reasonable to propose that XGS and CGS are worth a closer look despite their relatively high capital cost compared to EGS. Most crucially, XGS and CGS with their high operating flow rates in the range of 0.08 to 0.55 m^3/s will require large-diameter wells (e.g., >0.3 m) which will afford the space for more complex in-well tools. This implies that in-well flow proportioning tools could be achievable. As a reminder, this is a forecasting study for a greenfield site using almost no site-specific data and ultra-high subsurface uncertainty. As more data becomes available, the conclusions are likely to change. However, the idea that AGS could become more profitable than the alternatives seems exceptionally unlikely.

If we reach out one step further, we can extrapolate the XGS concept to a grid pattern of 4-XGS that share boundary wells. Now, the total number of wells would be 13 in order to generate the same amount of power as 4 XGS. Using this cost scaling factor of 13:4:5 (i.e., 0.65), we can estimate the nominal potential of 114 $/MWh for patterned XGS (i.e., 4XGS), which would be competitive with some of the cheapest energy technologies, including commercial-scale photovoltaics (i.e., Solar PV - Commerical). If the Wattenberg proves to have a higher temperature gradient than we can forecast without site-specific data (e.g., 50 °C/km), economic viability would increase for all of the above geothermal development methods.

7. CONCLUSIONS

We completed an ensemble of 40,000 reservoir scale simulations of drilling, stimulation, circulation, heat production, power production, and economic valuation in order to optimize and compare strategies for geothermal development in the Wattenberg geothermal anomaly. The data used to complete this work included essentially nothing other than the fundamental understanding of subsurface processes and what is physically possible. Clearly, this analysis does not yield a precise and accurate prediction, but it does elucidate a path forward and it reveals a multitude of useful insights. First, caged fracture systems hold promise for unlocking significantly more energy resources than was previously considered possible (e.g., 100 MWe for 15 years would be possible using a 2 km cube of hot rock). Second, 5-well caged EGS (i.e., XGS) hold promise to harvest geothermal energy safely and economically. Third, more stages is better for EGS, CGS, and XGS while in-well flow proportioning could help to achieve peak performance by better combating thermal short-circuiting. Fourth, natural fractures and shear stimulation tend to cause problems for design optimization via seismic risk and thermal short-circuits, so hydraulic shearing is unlikely to be effective for hot dry rock reservoir stimulation and it could be better to simply plug shear fractures. Fifth, AGS will require an enormous amount of drilling relative to its power output, so the likelihood that this technology could become cost competitive is low, especially given that a 90% reduction in drilling cost would benefit all subsurface technologies, including oil and gas.

ACKNOWLEDGEMENTS

This work is supported by Department of Energy (DOE) Basic Energy Sciences under FWP LANLE3W1. Additional support was provided by the Los Alamos National Laboratory's Laboratory Directed Research and Development – Exploratory Research program (LDRD-ER-20220175ER) and the DOE Geothermal Technologies Office (GTO) funded project – Geothermal Limitless Approach to Drilling Efficiencies (GLADE; DE-EE0010444) led by Oxy USA, Inc. We are grateful for this funding provided by DOE and LANL. The PIVOT 2022 and PIVOT 2023 Geothermal Datathons, co-organized by GTO and Society of Petroleum Engineers (SPE) were also instrumental for the completion of this work by revealing data analysis approaches that differed from our own. The views expressed herein do not necessarily represent the views of the U.S. Department of Energy of the United States Government.

REFERENCES

Duchane, D., Brown, D.: Hot Dry Rock (HDR) Geothermal Energy Research and Development at Fenton Hill, New Mexico, GHC Bulletin, December, 13-19 (2002).

Förster, A., and D. F. Merriam.: Heat flow in the Cretaceous of northwestern Kansas and implications for regional hydrology: Current Research in Earth Sciences, v. 240, (1997), 1-11.

Frash, L.P.: GeoDesignTool – GeoDT, GitHub, (2021), https://github.com/GeoDesignTool/GeoDT.

Frash, L.P.: Geothermal Design Tool (GeoDT), Proceedings, 46th Workshop on Geothermal Reservoir Engineering, Stanford University, Stanford, CA (2021).

Frash, L.P.: Optimized Enhanced Geothermal Development Strategies with GeoDT and Fracture Caging, Proceedings, 47th Workshop on Geothermal Reservoir Engineering, Stanford University, Stanford, CA (2022).

Frash, L.P., Carey, J.W., Ahmmed, B., Meng, M., Sweeney, M., K C, B., Iyare, U.: A proposal for Profitable Enhanced Geothermal Systems in Hot Dry Rock, Proceedings, 48th Workshop on Geothermal Reservoir Engineering, Stanford University, Stanford, CA (2023).

Frash, L.P., Fu, P., Morris, J., Gutierrez, M., Neupane, G., Hampton, J., Welch, N., Carey, J.W., Kneafsey, T.: Fracture Caging to Limit Induced Seismicity, Geophysical Research Letters, 48(1), e2020GL090648 (2020).

Frash, L.P., Li, W., Meng, M., Carey, J.W., Sweeney, M.: Enhanced Geothermal System Design Using GeoDT and Fracture Caging — EGS Collab Stimulation Prediction Study, Proceedings, 56th US Rock Mechanics/Geomechanics Symposium, Santa Fe, NM (2022).

Frash, L.P., Sweeney, M., Meng, M., K C, B., Iyare, U., Madenova, M., Carey, J.W., Li, W.: Exploring the Limitations of Fracture Caging in NextGen Enhanced Geothermal Systems, Proceedings, 57th US Rock Mechanics / Geomechanics Symposium, Atlanta, GA (2023).

Heidbach, O., M. Rajabi, X. Cui, K. Fuchs, B. Müller, J. Reinecker, K. Reiter, M. Tingay, F. Wenzel, F. Xie, M. O. Ziegler, M.-L. Zoback, and M. D. Zoback.: The World Stress Map database release 2016: Crustal stress pattern across scales. Tectonophysics, (2018), 744, 484-498.

Lazard: *Lazard's Levelized Cost of Energy Analysis*, (2019), Version 13.0.

Thul, D.J.: Niobrara source rock maturity in the denver basin: a study of differential heating and tectonics on petroleum prospectivity using programmed pyrolysis. Colorado School of Mines, Master's Thesis, (2012).